Article ID: 1001-3555(2019)01-0027-14

Fluorinated TS-1 Prepared by Microwave Irradiation and Its Catalytic Performance on Ammoximation of Cyclohexanone

XUE Xiao-lu[1], GAO Peng-fei[1*], ZHANG Lei[1], ZHAO Yong-xiang[2*]

(1. *School of Chemical and Chemical Engineering, Shanxi University, Taiyuan* 030006, *China*;
2. *Research Centre for Fine Chemical Engineering, Shanxi University, Taiyuan* 030006, *China*)

Abstract: Fluorinated TS-1 (F-TS-1-M) were prepared by treating TS-1 in dimethyl sulfoxide solution of sodium fluoride under the assistance of microwave in this work. The characterization results showed that F-TS-1-M presented increased amount of tetrahedral framework Ti thanks to the selective effect of microwave irradiation on activating M-O bonds with different dipole moments which could lead to the transformation of non-framework Ti^{4+} to framework Ti^{4+}. In addition, F-TS-1-M exhibited stronger Lewis acidity and hydrophobicity due to the reduced skeleton defects and surface hydroxyls. As a result, F-TS-1-M showed enhanced catalytic activity in the ammoximation of cyclohexanone.

Key words: fluorinated TS-1; microwave irradiation; lewis acidity; hydrophobicity; ammoximation

CLC number: O643.36 **Document code**: A

Since invented in 1983[1], titanium silicalite-1 (TS-1) has become one of the most attractive catalytic materials in the past few decades thanks to its excellent catalytic performance in the selective oxidation of organic compounds with dilute hydrogen peroxide as an oxidant under mild liquid-phase reaction conditions[2-8]. It has been reported that the essential of this catalytic oxidation by titanosilicate zeolite is the activation of H_2O_2, where tetrahedral framework Ti^{4+} sites are considered as the active sites. This implies that the catalytic activity of TS-1 could be improved by changing the electropositivity around the tetrahedral Ti^{4+}[9-10].

It has been reported that the electropositivity of the Ti^{4+} species could be strengthened by implanting fluorine, the most electronegative element, into a titanosilicate zeolite framework[9-11]. The fluorine species have been incorporated into the zeolite skeleton by direct synthesis in fluoride media or by post-treatment with fluoride salts[9-12]. Fluorinated Ti-MWW (F-Ti-MWW) was synthesized through acid treatment of Ti-MWW in the presence of ammonium fluoride[9,11-12]. The incorporated fluorine species significantly improved the catalytic performance of Ti-MWW in the epoxidation of alkenes, which could be attributed to the enhanced Lewis acid strength and the hydrophobicity of the zeolite[9,11-12]. Fluorine implanted Ti-MOR catalysts have been successfully synthesized by treating Ti-MOR with fluoride salts in water or methanol, and exhibited enhanced catalytic activity in ammoximation[10]. In contrast to these, there are few works on dealing with fluorinated TS-1[13]. Furthermore, these works just investigated the influence of fluorination on the catalytic activity of TS-1 while its impacts on the structure were scarcely involved. Owning to its importance in many selective oxidation reactions[2-7], the research on fluorination of TS-1 will provide new strategies to regulate its physical and chemical properties.

High-speed synthesis under microwave irradiation has attracted considerable attention in recent years, because microwave heating technique frequently leads to shorter reaction time, higher yield, and cleaner reaction profile owing to its dielectric heating and selective heating nature[14-15]. Microwave irradiation heating is uniquely capable of generating extremely high tempera-

Received date: 2018-12-09; **Revised date**: 2019-01-07.

Foundation: The financial supports from the National Natural Science Foundation of China (Project NO. 21403135), and Shanxi provincial key research and development plan project (NO. 201603D121018-1) are gratefully acknowledged.

First author: XUE Xiao-lu (1991-), famale, master.

Corresponding author: Gao Pengfei (1982-), male, doctor, heterogeneous catalysis, E-mail: pfgao@sxu.edu.cn.

tures in specific regions of the sample while maintaining lower temperatures in others[16]. This principle is widely used in the specific heating of active sites in supported metal catalysts[16-17]. There are several reports on the application of microwave irradiation during the synthesis of various zeolites[18-19]. For the microwave assistant synthesis of heteroatom zeolites, Cundy *et al.* did pioneering works including TS-1 and TS-2 synthesis[18]. There were reports on applications of the microwave method for the fabrication of MFI-type zeolite crystals incorporating Ti and other metal species[20].

In view of the specific advantages of microwave irradiation in zeolites preparation[14-21], fluorination of TS-1 (F-TS-1-M) was carried out under the microwave irradiation in this work. The catalytic performance of F-TS-1-M was investigated in cyclohexanone ammoximation, a green process for the production of cyclohexanone oxime[22]. For comparison, TS-1-M (TS-1 treated under microwave irradiation without the presence of fluoride salts) and F-TS-1-T (fluorinated TS-1 synthesized by traditional methods)[10,12] were also synthesized and used as catalysts for cyclohexanone ammoximation. All the synthesized catalysts were characterized by various techniques, e.g. X-ray diffraction, DR UV-Visible spectrophotometer, X-ray photoelectron spectroscopy, pyridine FT-IR spectrometer, N_2 adsorption, thermal gravity analysis, ^{19}F MAS NMR spectroscopy and ^{29}Si MAS NMR spectroscopy etc. Finally, the structure-activity correlations were studied.

1 Experimental

1.1 Catalyst preparation

1.1.1 Fluorination of TS-1 under microwave irradiation The TS-1 powder (Si/Ti = 25-30, Nanjing XFNANO Materials Tech Co. Ltd) was treated in dimethylsulfoxide (DMSO)/NaF solution at the 373 K for 1 h with Si/F=48 molar ratio and a solid-to-liquid ratio of 1.0 g to 20.0 g in a microwave reactor. The product was filtered, washed, and dried at 353 K for 12 h. The products were designated as F-TS-1-M.

For comparison, a bared sample was prepared according to the aforementioned procedures except the inexistence of NaF. The obtained product was designated as TS-1-M.

1.1.2 Fluorination of TS-1 via traditional method For comparison, fluorination of TS-1 was carried out according to the procedure reported in the literature[10,12,23]: The TS-1 powder was treated in methanol containing NaF (Si/F molar ratio of 48) with a solid-to-liquid ratio of 1.0 to 20.0 g at 373 K for 6 h in a Teflon-lined autoclave under magnetic stirring. The product was filtered, washed, and dried at 353 K for 12 h. The sample obtained was denoted as F-TS-1-T.

1.2 Characterization methods

XRD data were collected on aBruker D8 Advanced instrument using Cu Kα radiation at a beam voltage of 40 kV and a 40 mA beam current. The amount of framework Ti (x) was evaluated by measuring the cell volume and using the following empirical equation[22]: $V = 2093x + 5335.8$ Å^3. The cell volume of the samples dehydrated at 120 ℃ was extracted by full-profile analysis of XRD collected on a laboratory Bruker D8 instrument. Diffuse-reflectance UV-Vis spectra were collected using an Agilent Cary Win UV-300 UV-Vis spectrophotometer in 200~800 nm range. For each test with double beam mode and a $BaSO_4$ plate as the reference. The nitrogen adsorption and desorption isotherms were measured on a Micromeritics ASAP 2020 instrument. Prior to the adsorption measurements, the samples were outgassed at 423 K for 6 h under vacuum in order to remove absorbed water and other adsorbed species. ^{29}Si MAS NMR and experiments were performed on a Bruker AVANCE III 600 spectrometer at a resonance frequency of 119.2 MHz. ^{29}Si MAS NMR spectra with high power proton decoupling were recorded on a 4 mm probe with a spinning rate of 10 kHz, a π/4 pulse length of 2.6 s, and a recycle delay of 80 s. The chemical shift of ^{29}Si was referenced to TMS. ^{19}F MAS NMR experiments were carried out on a Bruker AVANCE III 600 spectrometer at a resonance frequency of 564.5 MHz using a 4 mm HX double-resonance MAS probe at a sample spinning rate of 14 kHz. ^{19}F MAS NMR spectra were recorded on a 4 mm probe with a π/2 plus length of 3.5 μs and a 5 s recycle delay. The chemical shifts of ^{19}F was referenced to PTFE. X-ray photoelectron spectroscopic (XPS) were performed

on a Thermo Fisher Scientific spectrometer equipped with a conventional Al-Kα nonmonochromatized source. For pyridine spectra measurement, a self-supported wafer (1.2 cm in diameter) was set in a quartz IR cell sealed with CaF_2 windows connected with a vacuum system. After the sample was evacuated at 723 K for 1.5 h, pyridine adsorption was carried out by exposing the wafer to pyridine vapor at 323 K for 0.5 h. The absorbed and chemisorbed pyridine was then removed by evacuation at different temperatures (323~523 K) for 0.5 h. All the spectra were collected at room temperature. The spectra of hydroxyl stretching were measured on self-supported wafers. The wafer was set in a quartz cell which was sealed with CaF_2 windows and connected to a vacuum system. After the sample was evacuated at 723 K for 1 h, the spectra were recorded in absorbance mode at room temperature. Thermo gravimetrical analysis (TG) was performed on a Shimadzu TGA-50 instrument with an air flow rate of 30 mL/min. The samples were heated from ambient temperature to 523 K with a heating rate of 10 K/ min. The amounts of titanium of all samples were analyzed on a Rigaku ZSX-100e X-ray fluorescence spectrometer (XRF, Japan).

1.3 Catalytic tests

1.3.1 The decomposition of free H_2O_2　The decomposition reaction of free H_2O_2 was carried out to determine the apparent activation energy of formed Ti-OOH active species over catalysts[24]. In a typical process, 5.0 g of catalyst and 40 mL solvent (CH_3OH) were well mixed in the reactor. When the temperature of slurry reached the desired value (318, 328 and 333 K), the reaction was initiated by introducing 10 mmol H_2O_2 (30% (weight percentage)). Then the reaction proceeded for another 5 min, and the residual free H_2O_2 concentration was determined by indirect iodometry. The relevant activation energy was calculated using Arrhenius equation ($k = Aexp(-E_a/RT)$).

1.3.2 Ammoximation of cyclohexanone/benzaldehyde

The catalytic activity of zeolite materials obtained above was evaluated in cyclohexanone/benzaldehyde ammoximation. The reaction was carried out in a 25 mL three-neck glass flask equipped with the magnetic stirrer and a condenser. Typically, 0.5 g catalysts and 1.0 g cyclohexanone/benzaldehyde were added into a flask with 1.7 g distilled water and 1.7 g *tert*-butanol. Then, the mixture was heated to 353 K. The reaction was started immediately by the addition of 3.7 g aqueous NH_3-solution (30% (weight percentage)) and 3.9 g of H_2O_2 (30% (weight percentage)) into the flask dropwise, respectively. After complete addition of H_2O_2 and NH_3-solution within 1 h, the mixture continued to react for another hour. The reaction products were analyzed by a gas chromatograph (Agilent 7890B) equipped with an FID detector.

Catalytic recycles were carried out to investigate the catalytic stability of the catalysts. After the reaction, the catalysts were filtered, washed with methanol 5 times, and dried at 353 K under vacuum. For the next run, all of them were weighed and reused under the same conditions.

2 Results and discussion

2.1 Characterization

To investigate the effects of fluorination on the skeleton structure, the crystalline phase of parent and fluorine modified TS-1 zeolites are characterized by powder XRD and the results are shown in Fig.1. It can

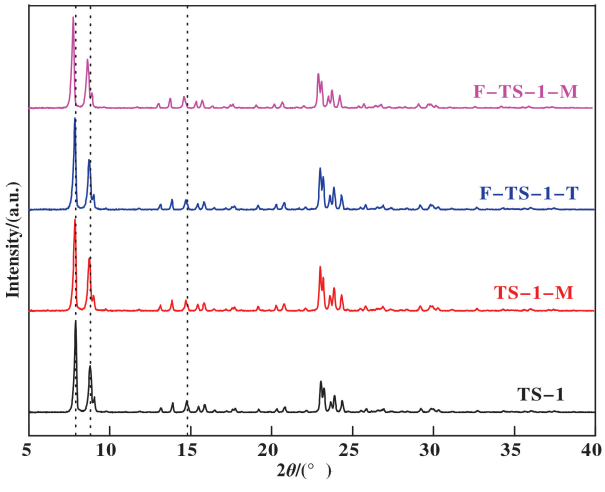

Fig.1 XRD patterns of TS-1, TS-1-M, F-TS-1-T and F-TS-1-M

be seen that all samples show typical MFI diffraction peaks as reported in the literature[25]. In comparison to TS-1, the cell volume and framework Ti content of F-TS-1-T (Table 1) decreased, indicating some

Table 1 The relativecrystallinity, cell volumes, and deduced framework Ti contents [22] for TS-1, TS-1-M, F-TS-1-T and F-TS-1-M

Catalysts	Relative crystallinity [a]	Cellvol ($Å^3$) [b]	Ti content (atoms/cell) [c]	Ti amounts /% [d]
TS-1	1.00	5379.9	2.11	2.02
TS-1-M	1.25	5385.3	2.36	2.02
F-TS-1-T	1.22	5379.2	2.07	2.03
F-TS-1-M	1.29	5393.2	2.73	2.05

a. calculated according to the peak intensity of TS-1-M, F-TS-1-T and F-TS-1-M to the intensity of the TS-1;

b. calculated according to the samples dehydrated at 120 ℃ was extracted by full-profile analysis of XRD collected on a laboratory Bruker D8 instrument;

c. calculated according to the following empirical equation [22]: $V = 2093x + 5335.8$ $Å^3$;

d. determined by XRF method.

framework Ti transferred to non-framework ones which may be caused by Si—O—Ti bond cleavage in methanol due to bond polarization[26]. In contrast to this, all diffraction peaks of F-TS-1-M and TS-1-M shift to small angles, which demonstrates large atoms (Ti) have entered into the zeolite framework[27]. Namely, some non-framework Ti species of F-TS-1-M and TS-1-M have been transformed to framework ones during modification process, which is confirmed by the fact that the cell volume and framework Ti content (Table 1) of these two samples increased compared to TS-1. This phenomenon is ascribed to the selective effects of microwave[19,28]. Due to their higher dipole moment ($D_e = 2.18$) than Si-O ($D_e = 1.76$), Ti-O bonds on the TS-1 surfaces can be strongly activated by microwave irradiation and undergo condensation reactions to form Ti—O—Ti and/or Ti—O—Si bonds[18,29]. It can be seen from Table 1 that all the modified samples show higher relative crystallinity[19,28] than TS-1, indicating less defects in their skeletons[30]. We can also see from Table 1 that these samples possess almost same titanium amounts. Combined with XRD results, it can be concluded that titanium species were not recrystallized under microwave irradiation conditions.

The coordination state of titanium is determined by ultraviolet diffuse reflectance spectroscopy (DR UV-Vis)[31]. Fig.2A shows the DR UV-Vis spectra of modified and unmodified TS-1 samples. Multibands are

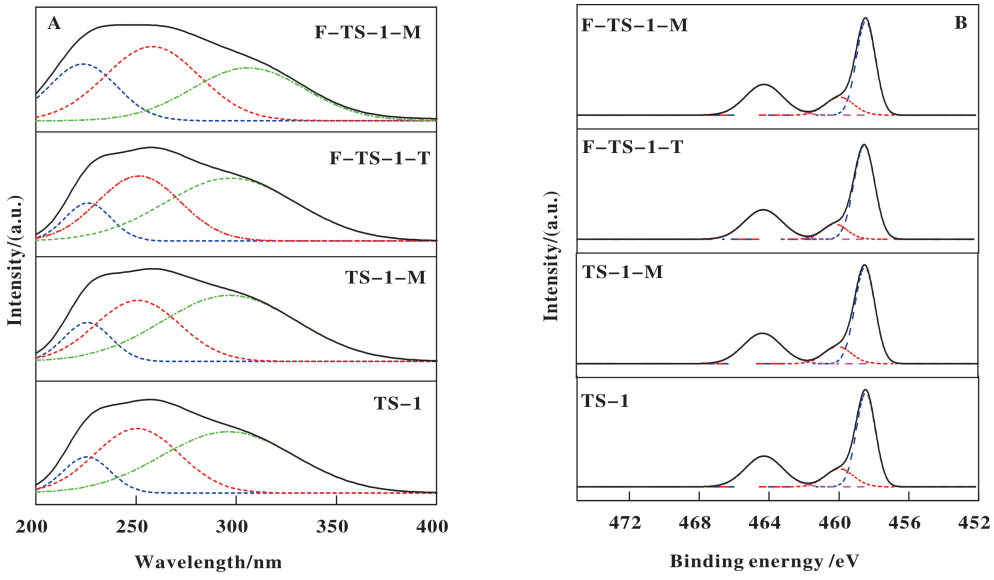

Fig.2 DR UV-Vis (A) and XPS (B) spectra of TS-1, TS-1-M, F-TS-1-T and F-TS-1-M

deconvoluted by the Peak Fit program using the Gaussian fitting method[32]. All samples exhibit three major bands sited at 210～230, 240～260, and 300～310 nm. The band at 210～230 nm is usually ascribed to a charge transfer between tetrahedral-coordinated Ti^{4+} and O^{2-} of the TS-1 zeolite framework and thus is assigned to framework Ti[10,32-33]. The band at about 240～260 nm is considered as a charge transfer process in non-framework Ti species (isolated [TiO_4] or [HO-TiO_3] units), while the band at 300～310 nm is ascribed to anatase TiO_2[32-33]. It is worth noting that the F-TS-1-M sample has a stronger band at 210～230 nm than other examined samples, indicative of the highest framework Ti content in F-TS-1-M. In contrast, the band at 240～260 nm from of F-TS-1-M is less obvious than those of TS-1, TS-1-M and F-TS-1-T, indicating low non-framework Ti amount in F-TS-1-M. The relative content of different types of Ti are calculated according to C. Xia *et al.*, and the results are listed in Fig.3[32]. Obviously, the framework Ti content of TS-1-M are higher than those of TS-1 and F-TS-1-T. The DR UV-Vis results indicate that microwave irradiation can promote the transformation of non-framework Ti to framework Ti and consolidate in further the XRD findings.

The samples were analysed by XPS to determine the surface elemental composition and electronic state of Ti. After deconvolution[34-35], the spectra (Fig.2B) of all catalysts demonstrate two Ti $2p_{3/2}$ peaks at about

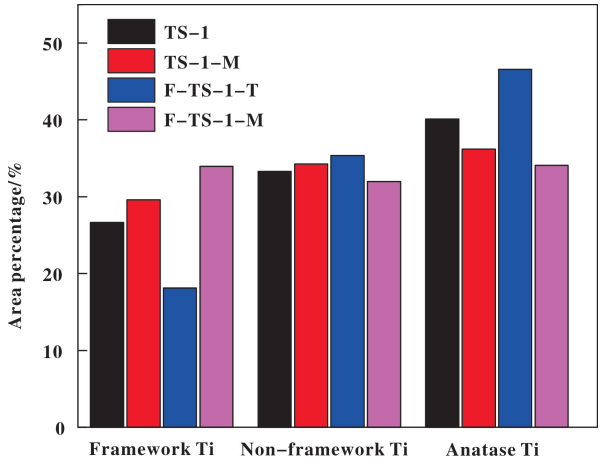

Fig.3 The corresponding distributions of framework Ti species (at 210～230 nm), non-framework Ti species (at 240～260 nm), and anatase TiO_2 (at 300～310 nm) in TS-1, TS-1-M, F-TS-1-T and F-TS-1-M

459.7 and 458.4 eV, which are assigned to titanium in tetrahedral and octahedral coordination respectively[34-36]. The ratios of the tetrahedral Ti^{4+} to octahedral Ti^{4+} (Ti^{4+}(t)/Ti^{4+}(o)) are summarized in Table 2. Compared with TS-1, Ti^{4+}(t)/Ti^{4+}(o) of F-TS-1-M increased and that of F-TS-1-T decreased, demonstrating that fluorination by microwave irradiation has transformed some octahedral Ti to tetrahedral Ti while some tetrahedral Ti were transferred to octahedral Ti during NaF post-treatment in methanol. The XPS results (Table 2) also show that F-TS-1-M and F-TS-1-T have similar surface fluorine contents.

Table 2 The Ti^{4+}(t)/ Ti^{4+}(o) (tetrahedral to octa-hedral Ti^{4+}), surface atomic concentration, and relative amounts of Q^3 and Q^{4*} Si of different catalysts

Catalysts		TS-1	TS-1-M	F-TS-1-T	F-TS-1-M
Ti^{4+}(t)/ Ti^{4+}(o)[a]		0.26	0.28	0.19	0.29
Surface atomic concentration[b]	Si	41.3%	41.1%	41.0%	40.8%
	F	–	–	1.4%	1.6%
The amounts of Q^3Si[c]		11.4%	2.8%	3.0%	2.6%
The amounts of Q^{4*} Si[d]		36.8%	36.9%	36.2%	38.2%

a. calculated according to deconvolution results of Ti 2*p* XPS;

b. calculated according to the XPS results;

c. calculated by $Q^3/(Q^3+Q^4+Q^{4*})$ according to the deconvolution results of ^{29}Si MAS NMR;

d. Si of Si-O-Ti bonds, calculated by $Q^{4*}/(Q^3+Q^4+Q^{4*})$ according to the deconvolution results of ^{29}Si MAS NMR.

^{19}F MAS NMR spectroscopy (Fig.4) was employed to identify the Si-F species generated in F-TS-1-M and F-TS-1-T. Both samples exhibit resonances at −72, −122, and −147 ppm. The resonance at −72 ppm is attributed to the fluoride occurring as ion pairs and the −147 ppm was ascribed to Si-F bond[9,37]. The −122 ppm resonance is attributed to SiF_6^{2-} species[10,12]. The ^{19}F MAS NMR spectrum verified that the F species are incorporated into F-TS-1-M and F-TS-1-T successfully via forming Si—F bonds and the F^- presented as SiF_6^{2-} species.

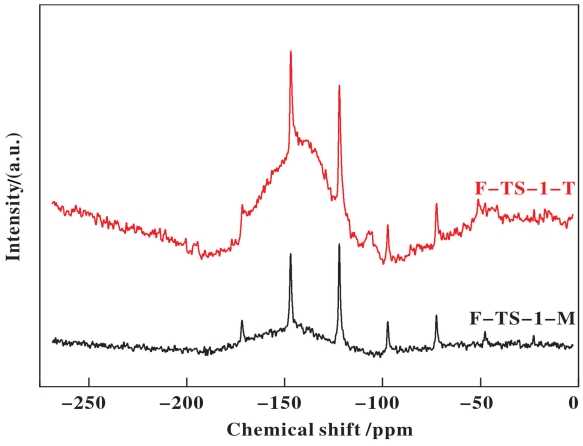

Fig.4 ^{19}F MAS NMR spectra of F-TS-1-M and F-TS-1-T

^{29}Si MAS NMR spectroscopy was used to investigate the effects of fluorination on the amounts of Si-OH groups and structure defects. As depicted in Fig.5, all samples show a strong peak at −113 ppm and a weak peak at −103 ppm, which are assigned to $Si(OSi)_4$ (Q^4) featured with a perfect symmetry with Si—O—Si bands and $Si(OSi)_3OH$ (Q^3) species, respectively[9,38-39]. A calculation of deconvoluted spectra show that the Q^3 percentages are 11.4%, 2.8%, 3.0%, and 2.6% for TS-1, TS-1-M, FTS-1-T and F-TS-1-M, respectively (Table 2). The decreased Q^3 percentages indicate that fluorination partially removed the hydroxyl groups of TS-1[9,12] via forming Si-F bonds and reduced the structure defects[30,40] which has been verified by the relative crystallinity of samples. In addition, a shoulder peak (Q^{4*}) of Q^4 appeared at about −117 ppm, which result from the distortion of Si-O-Ti via the

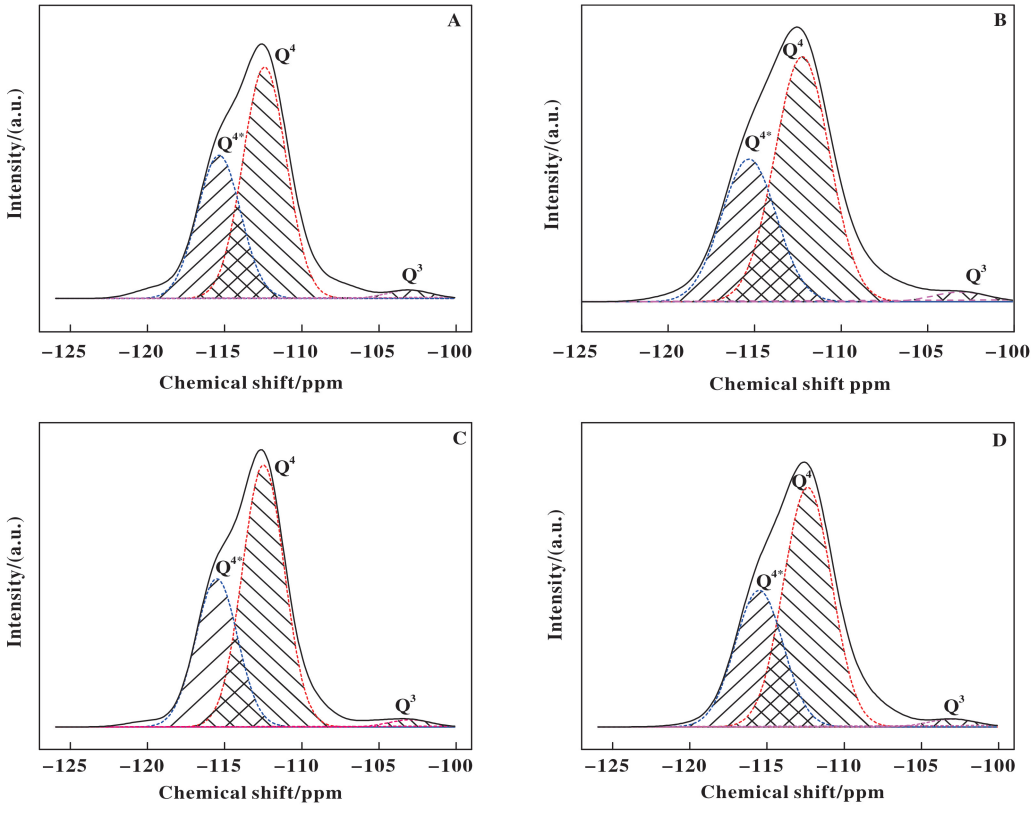

Fig.5 ^{29}Si MAS NMR spectra of TS-1 (A), TS-1-M (B), F-TS-1-T (C) and F-TS-1-M (D)

insertion of Ti leading to a less symmetry in Q^4[41,44]. The percentages of Q^{4*} are 36.8%, 36.9%, 36.2% and 38.2% for TS-1, TS-1-M, F-TS-1-T and F-TS-1-M, respectively, suggesting that fluorination via microwave irradiation promoted the Si—O—Ti bonds formation while fluorination by post-treatment of NaF in methanol broke the Si—O—Ti bonds which is consistent with DR UV-Vis results.

N_2 adsorption was carried out to investigate effects of fluorination on the texture properties of these catalysts. Fig.6 shows the N_2 sorption isotherms of TS-1, TS-1-M, F-TS-1-T and F-TS-1-M. It can be seen that all samples present a hysteresis loop resembling H2-type, indicating nonuniform cylindrical pore shapes[10,34,42]. In comparison to TS-1, the micropore volumes, pore diameters and specific surface areas (Table 3) of F-TS-1-T and F-TS-1-M decreased . The somewhat larger decreased porosity of F-TS-1-T can be ascribed to the pore blocking caused by formation of non-framework Ti species during the fluorination process which has been evidenced by XRD, UV-Vis, and XPS. As to F-TS-1-M, the slightly decreased porosity may result from the reduced structure defects caused by condensation of Ti-OH and Si-OH during microwave irradiation which had been verified by NMR and FT-IR etc. Unlike F-TS-1-M and F-TS-1-T, the pore diameter and specific surface area of TS-1-M increased while the micropore volume decreased in comparison to TS-1.

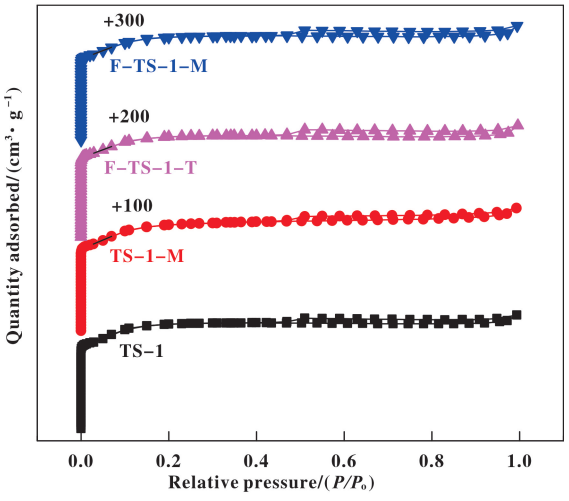

Fig.6 N_2 adsorption-desorption isotherms of TS-1, TS-1-M, F-TS-1-T and F-TS-1-M

Table 3 Physicochemical properties of TS-1, TS-1-M, F-TS-1-T and F-TS-1-M

Catalysts	S_{BET} /($m^2 \cdot g^{-1}$)	V_{micro} /($cm^3 \cdot g^{-1}$)	Pore diameter /nm
TS-1	346	0.131	0.845
TS-1-M	355	0.124	0.858
F-TS-1-T	333	0.126	0.840
F-TS-1-M	343	0.129	0.843

It has been reported that an oxidation process that requires the simultaneous presence of nonpolar and polar (H_2O_2 aq) reactants within the zeolite pores, the hydrophobicity /hydrophilicity of the catalyst will play an important role[9-12]. Thus, the hydrophobicity/ hydrophilicity of the catalysts was characterized by FT-IR and TG. Fig.7 presents the IR spectra in the hydroxyl stretching vibration region (3000~4000 cm^{-1}) for TS-1, TS-1-M, F-TS-1-T, and F-TS-1-M. The spectra are measured after removal of water by evacuation at 573 K. The parent TS-1 exhibits an intense adsorption band at 3720 cm^{-1} and a broad band centered at 3520 cm^{-1}, ascribed to terminal silanol groups and hydroxyl nests, respectively[43-44]. Besides the 3720 and 3520 cm^{-1} bands, F-TS-1-T exhibits a new band at 3640 cm^{-1}, which is assigned to the Gemini-type silanol groups and resulted from the transformation of framework Ti to non-

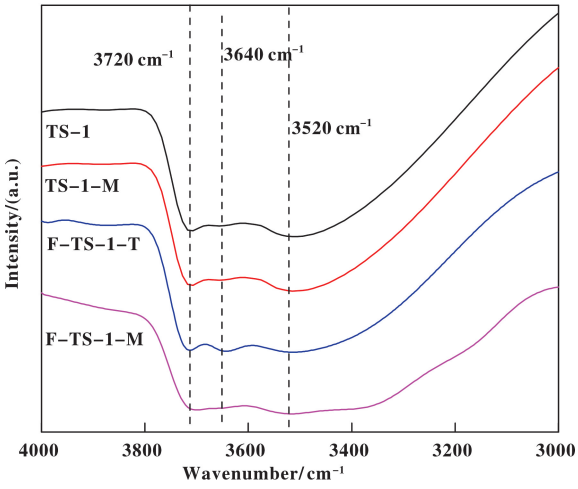

Fig.7 IR spectra of TS-1, TS-1-M, F-TS-1-T and F-TS-1-M

framework Ti by cleavage of Ti—O—Si bonds as evidenced by DR UV-Vis and ^{29}Si MAS NMR spectra. In addition, TS-1-M exhibits similar spectrum to TS-1, indicating microwave irradiation had little slight influence on the amounts of surface hydroxyls. In the case of F-TS-1-M, the intensity of 3720 and 3520 cm^{-1} bands decrease to some extent, implying the decreased structure defects and surface hydroxyls, which had been confirmed by NMR spectra[9]. Thus F-TS-1-M is more hydrophobic than TS-1, TS-1-M and F-TS-1-T.

The hydrophobicity/hydrophilicity of TS-1, TS-1-M, F-TS-1-T and F-TS-1-M is further qualitatively determined by TG method according to the procedure reported in reference[45-46]. All samples were pretreated at 393 K to remove any adsorbed water, then equilibrated at room temperature with the water vapor supplied by the saturated solution of $MgCl_2$ for two days. As can be seen from Fig.8, TS-1 and F-TS-1-T exhibit a main

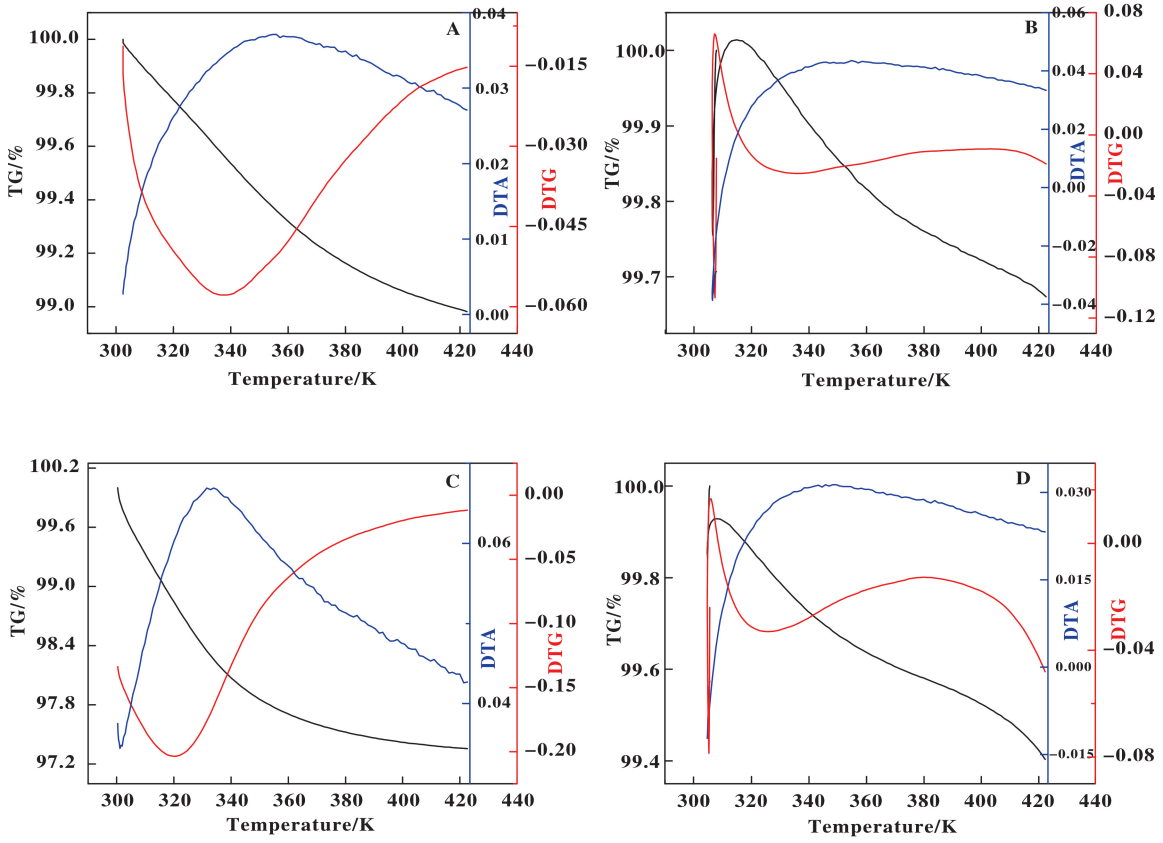

Fig.8 The TG, DTG, DTA of TS-1 (A), TS-1-M (B), F-TS-1-T (C) and F-TS-1-M (D)

weight loss in the range of 323~420 K corresponding to physical adsorbed water and amount to 1.2% and 2.5%, respectively. In addition, F-TS-1-M presents a weight loss about 0.5% in the range of 323~420 K corresponding to adsorbed water. The TG results demonstrate that F-TS-1-M is more hydrophobic and F-TS-1-T is less hydrophobic than TS-1.

Lewis acidity is another key factor influencing the selectivity of the oxime in ammoximation[12,24,44]. It has been reported that higher Lewis acidic strength of Ti can activate promote the formation of Ti-OOH species by reducing their activation energy[9-11,47]. Pyridine can be used as a probe molecule to provide more details on acid site's types, strength, and amount. Fig.9 shows the FT-IR spectra of adsorbed pyridine in the range of pyridine ring-stretching modes after desorption at various temperatures. All samples exhibit two distinct bands at 1604 and 1490 cm^{-1}, which are assigned to Lewis acid sites with a relatively high strength in TS-1[9,48-49]. Their intensity were calculated according to Z. Zhuo *et al.*[24], and the results were listed in Fig. 10. It can be seen that the acid strength of these cataly-

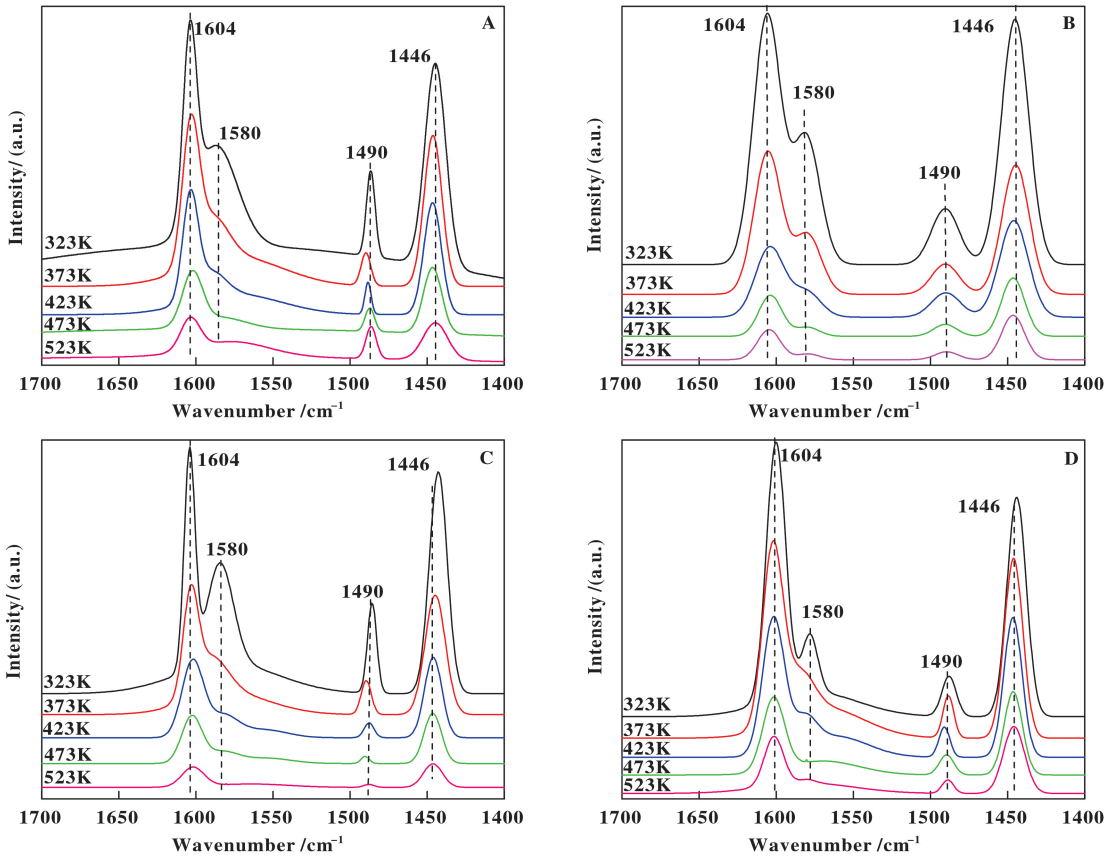

Fig.9 FT-IR spectra in the pyridine regions of TS-1 (A), TS-1-M (B), F-TS-1-T (C) and F-TS-1-M (D) at different evacuation temperatures

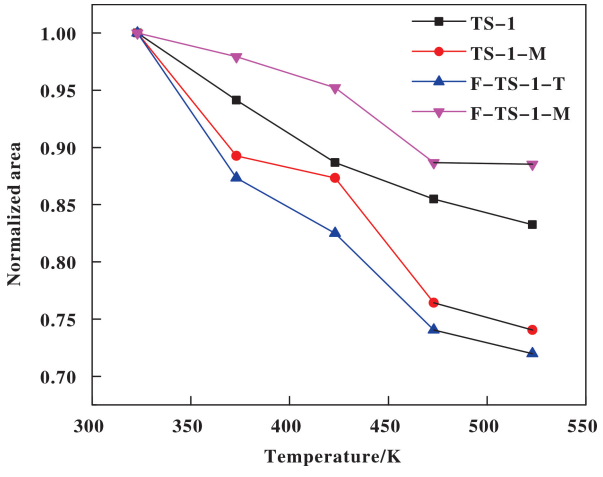

Fig.10 Correlation between the Lewis acidic strength of TS-1, TS-1-M, F-TS-1-T and F-TS-1-M

sis decreased in the order of F-TS-1-M > TS-1 > TS-1-M > F-TS-1-T, indicating F-TS-1-M has the highest Lewis acid strength. The spectra also show a shoulder band at 1580 cm^{-1} which is attributed to the vibrations of stretching modes of hydrogen-bonded and physically adsorbed pyridine and disappeared after desorption at 423 K[12,48-49]. Furthermore, the 1446 cm^{-1} band of all spectra, ascribed to hydrogen-bonded pyridines, remained after desorption at 523 K, demonstrating these samples had hydroxyl groups with moderate acidity[12,48-49]. These results verify that fluorination via microwave irradiation can strengthen the Lewis acidity of TS-1 due to the formation of Si-F species and the transformation of non-framework Ti to tetrahedral framework Ti species as proved by previous characterization methods[9,12]. On the contrary, F-TS-1-T exhibits reduced weak Lewis acidity compared with parent TS-1, which could be attributed to the transformation of tetrahedral framework Ti to non-framework Ti species via Ti-O-Si breakage. The apparent activation energies (E_a) of Ti-OOH active species formed on these zeolites are calculated by fitting the Arrhenius equation and were 31.6, 32.8, 50.6 and 19.8 kJ/mol for TS-1, TS-1-M, F-TS-1-T and F-TS-1-M, respec-

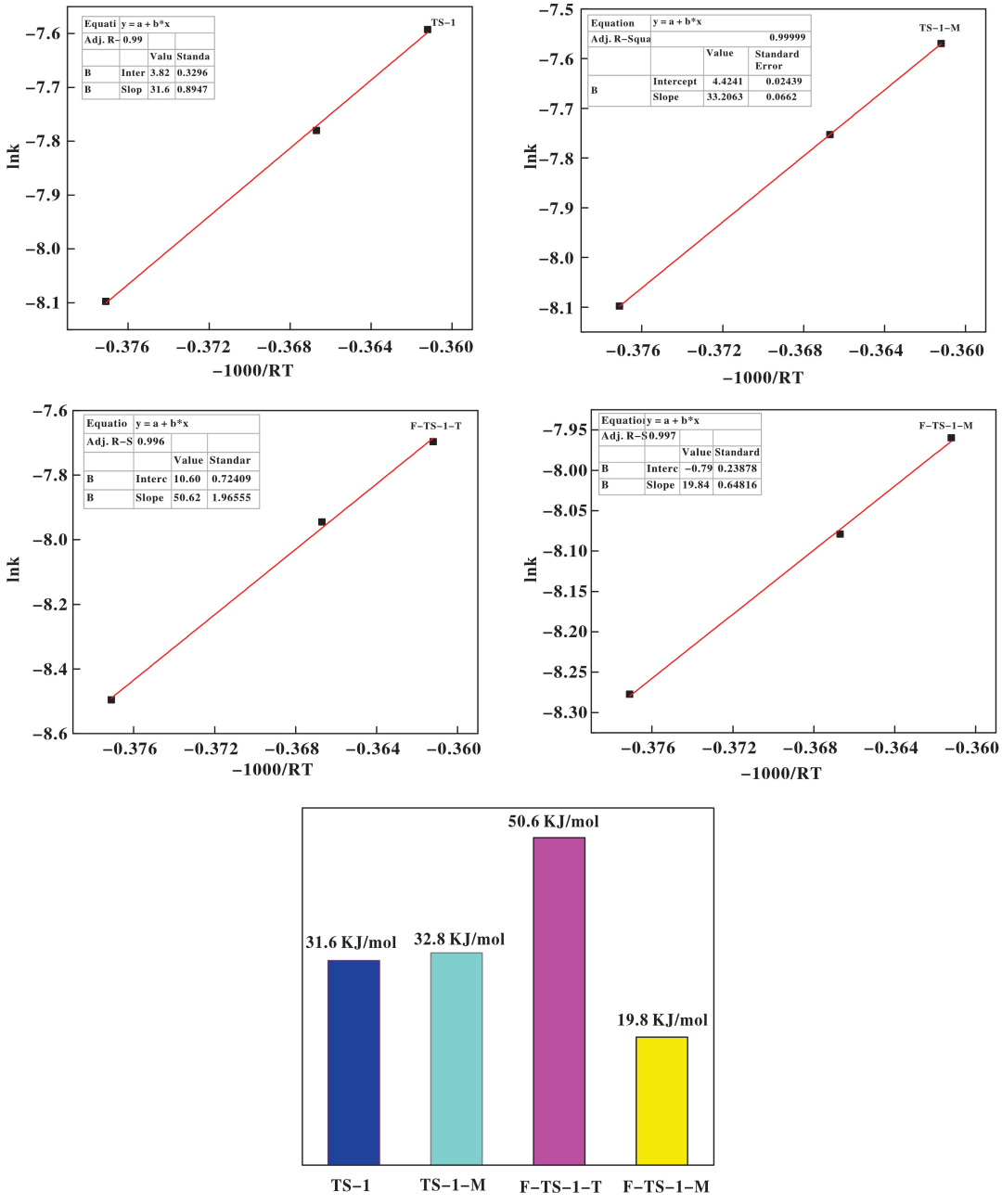

Fig.11Apparent activation energy (E_a) of formed active intermediates of Ti-OOH species over TS-1, TS-1-M, F-TS-1-T and F-TS-1-M.

tively (Fig.11)[24]. It can be concluded that F-TS-1-M with strongest Lewis acidity showed highest ability for activating H_2O_2, which would lead to high selectivity in ketone ammoximation[24].

2.2 Catalytic Ammoximation of Cyclohexanone

The catalytic activity these zeolites was investigated in the ammoximation of cyclohexanone and the results are listed in Table 4. It is obvious that F-TS-1-M exhibits the highest catalytic activity, which could be attributed to its high surface hydrophobicity, strong Lewis acidity as well as increased amount of framework tetrahedral Ti species. The high surface hydrophobicity favors the adsorption of reactants and desorption of product molecules from active sites. Additionally, the strong Lewis acidity can lower the activation barrier of free H_2O_2 and thus promote participation of free H_2O_2

Table 4 Ammoximation of cyclohexanone/ benzaldehyde

Catalysts	Ammoximation of cyclohexanone			Ammoximation of benzaldehyde		
	$X_{Cyclohexanone}$/%	S_{Oxime}/%	$S_{cyclohexylimine}$/%	$X_{Benzaldehyde}$/%	S_{Oxime}/%	$S_{benzoic\ acid}$/%
TS-1	94.9	87.7	12.3	96.8	85.7	14.3
TS-1-M	95.0	87.9	12.1	97.0	86.0	14.0
F-TS-1-T	86.5	80.1	19.9	100	78.3	21.7
F-TS-1-M	100	95.6	4.4	100	92.0	8.0

Reaction conditions: 0.5 g catalysts, 1.0 g cyclohexanone/benzaldehyde, 3.7 g aqueous NH_3-solution (30% (weight percentage)), 3.9 g H_2O_2 aqueous solution (30% (weight percentage)), 1.7 g H_2O, 1.7 g *tert*-butanol, reaction temperature 353 K, reaction time 2 h.

molecules in the formation of NH_2OH intermediates and inhibit side reactions caused by free H_2O_2. Furthermore, the increased framework tetrahedral Ti amount provide more active centers for ammoxiamtion reactions. Thus, F-TS-1-M shows enhanced cyclohexanone conversion and oxime selectivity. Additionally, TS-1-M shows similar cyclohexanone conversion and oxime selective to TS-1 demonstrating that microwave irradiation alone could not improve the catalytic activity of TS-1. In another word, the improved catalytic activity of F-TS-1-M stems from the combination effects of microwave irradiation and fluorination.

Catalytic recycles were carried out to investigate the catalytic stability of F-TS-1-M and the results were listed in Table 5. We can see that after 8 catalytic recycles, the cyclohexanone conversion and cyclohexnoane oxime are as high as those of the first run, demonstrating F-TS-1-M has high stability.

Table 5 Catalytic recycles of cyclohexanone ammoximation over F-TS-1-M

Catalytci runs	$X_{Cyclohexanone}$/%	S_{Oxime}/%
1	100	95.6
2	100	95.0
3	100	94.2
4	100	96.0
5	100	95.2
6	100	93.8
7	100	94.0
8	100	94.2

Reaction conditions: 0.5 g catalysts, 1.0 g cyclohexanone/benzaldehyde, 3.7 g aqueous NH_3-solution (30% (weight percentage)), 3.9 g H_2O_2 aqueous solution (30% (weight percentage)), 1.7 g H_2O, 1.7 g *tert*-butanol, reaction temperature 353 K, reaction time 2 h.

On the contrary, F-TS-1-T exhibits the poorest activity incyclohexanone ammoximation, which is in accordance with the results of previous reports[13]. The aforementioned characterization results demonstrate that F-TS-1-T presents reduced active tetrahedral framework Ti centers, weakened surface hydrophobicity and highest apparent activation energy (50.6 kJ/mol) of Ti-OOH active species, which leads to the decreased cyclohexanone conversion and oxime selectivity on F-TS-1-T.

The kinetics of ammoximation of cyclohexanone was studied over TS-1, TS-1-M, F-TS-1-T and F-TS-1-M in a temperature range of 323~353 K (Fig.12).

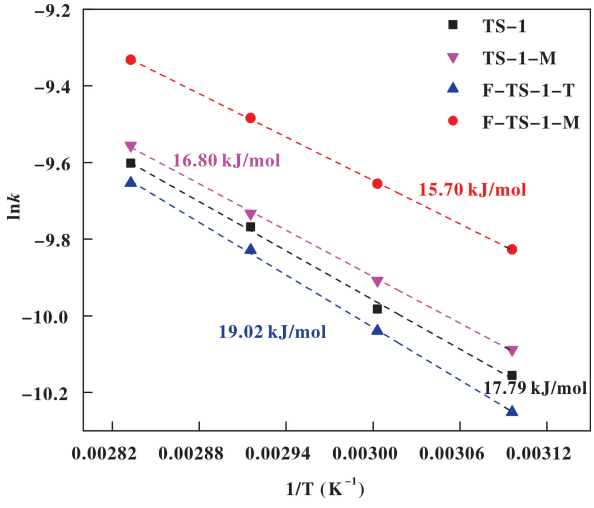

Fig.12 Plots of apparent activation energy in the ammoximation of cyclohexanone

The ammoximation of cyclohexanone is a first order reaction[50]. The apparent activation energies (E_a) calculated by fitting the Arrhenius equation[24,47], are 17.79, 16.80, 19.02 and 15.70 kJ/mol for TS-1, TS-1-M, F-TS-1-T and F-TS-1-M, respectively (Fig.12). Hence, it could be concluded that the fluorination with microwave irradiation lowered the apparent activation energy for the ammoximation of cyclohexanone through modifying the local chemical environment of the framework Ti sites, which resulted in increased oxidation reactivity[47].

The catalytic activity of these catalysts was also investigated in the ammoximation of benzaldehyde and the results were presented in Table 4. We can see that the catalytic activity of these catalysts showed the same trends as that in cyclohexanone ammoximation which consolidates in further that, fluorination under microwave irradiation can improve the catalytic activity of TS-1.

3 Conclusions

Fluorinated TS-1 has been successfully prepared via treating TS-1 with DMSO solution containing NaF under microwave irradiation. The XRD, DR UV-Vis, ^{29}Si NMR results showed that microwave irradiation could promote the transformation of non-framework Ti species to tetrahedral framework Ti due to the selective effect of microwave irradiation. The ^{19}F NMR showed that fluorine had been implanted into TS-1 framework by forming Si-F species which in turn led to the increase of hydrophobicity and Lewis acidity strength. As a result, the fluorinated TS-1 showed enhanced catalytic activity in the ammoximation of cyclohexanone and benzaldehyde.

References:

[1] Taramasso M, Perego G, Notari B. US [P], 4410501, 1983.

[2] Li H, Xu B, Deng B W, *et al.* Epoxidation of 1-hexene with hydrogen peroxide over nitrogen-incorporated TS-1 zeolite [J]. *Catal Commun*, 2014, **46**: 224-227.

[3] Ren Rong-xin (任容欣), Song Wan-cang (宋万仓), Liu Guan-feng (刘冠峰), *et al.* Recent research in preparation and application of hierarchical titanium silicalite-1 molecular sieve (多级孔钛硅分子筛的制备及应用进展) [J]. *J Mol Catal (China)* (分子催化), 2017, **31** (6): 594-604.

[4] Zhao Hong (赵 虹), Zhou Ji-cheng (周继承). Catalytic properties of titanium silicalite-1 prepared by mineral materials for the cyclohexanone ammoximation (无机钛硅原料合成 TS-1 对环己酮氨氧化的催化性能) [J]. *J Mol Catal (China)* (分子催化), 2003, **17**(3): 193-197.

[5] Zhang Jia-lin (张嘉霖), Sun Pei-yong (孙培永), Zhang Sheng-hong (张胜红), *et al.* Deactivation of TS-1 zeolites in the catalytic conversion of ethylene to ethylene glycol (乙烯催化转化制备乙二醇反应中 TS-1 分子筛的失活) [J]. *J Mol Catal (China)* (分子催化), 2015, **29**(3): 229-237.

[6] Zhang Hai-jiao(张海娇), Yao Ming-kai(姚明恺), Xie Wei(谢 伟), *et al.* Synthesis of TS-1 using inorganic SiO_2-TiO_2 precursor and its catalytic performance for hydroxylation of phenol(TS-1 分子筛的无机法合成及其催化苯酚羟基化性能) [J]. *Chin J Catal*(催化学报), 2007, **28**(10): 895-899.

[7] Wei Y, Li G, Qiang L, *et al.* Green and efficient epoxidation of methyl oleate over hierarchical TS-1 [J]. *Chin J Catal*, 2018, **39**(5): 964-972.

[8] Wu L Z, Tang Z M, Yu Y K, *et al.* Facile synthesis of a high-performance titanosilicate catalyst with controllable defective $Ti(OSi)_3OH$ sites [J]. *Chem Commun*, 2018, **54**(49): 6384-6387.

[9] Fang X, Sun L, Lin L, *et al.* Enhanced catalytic oxidation performance of F-Ti-MWW through the synergistic effect of anion and cation [J]. *Catal Commun*, 2017, **96**: 54-57.

[10] Yang Y, Ding J, Wang B, *et al.* Influences of fluorine implantation on catalytic performance and porosity of MOR-type titanosilicate [J]. *J Catal*, 2014, **320**(1): 160-169.

[11] Fang X, Wang Q, Zheng A, *et al.* Post-synthesis, characterization and catalytic properties of fluorine-planted MWW-type titanosilicate [J]. *Phy Chem Chem Phy*, 2013, **15**(14): 4930-7938.

[12] Fang X, Wang Q, Zheng A, *et al.* Fluorine-planted titanosilicate with enhanced catalytic activity in alkene epoxidation with hydrogen peroxide [J]. *Catal Sci Technol*, 2012, **2**(12): 2433-2435.

[13] Na K, Jo C, Kim J, *et al.* MFItitanosilicate nanosheets with single-unit-cell thickness as an oxidation catalyst u-

sing peroxides [J]. *ACS Catal*, 2011, **1**(8): 901-907.
[14] Bykov Y V, Rybakov K I, Semenov V E. High-temperature microwave processing of materials [J]. *J Phys D*, 2001, **34**(13): 55-75.
[15] Tao P, LuX, Zhang H, *et al.* Enhanced activity of microwave-activated CoO_x MOR catalyst for the epoxidation of α-pinene with air [J]. *Mol Catal*, 2019, **463**: 8-15.
[16] Zhang X, Hayward D O, Mingos D M P. Effects of microwave dielectric heating on heterogeneous catalysis [J]. *Catal Lett*, 2003, **88**(1/2): 33-38.
[17] Jamil A K, Muraza O, Miyake K, *et al.* Stable production of gasoline-ranged hydrocarbons from dimethyl ether over iron-modified ZSM-22 zeolite [J]. *Energ Fuel*, 2018, **32**(11): 11796-11801.
[18] Cundy C S, Forrest J O. Some observations on the preparation and properties of colloidal silicalites: Part II: preparation, characterisation and properties of colloidal silicalite-1, TS-1, silicalite-2 and TS-2 [J]. *Micro Mes Mater*, 2004, **72**(1): 67-80.
[19] Kitchen H J,Vallance S R, Kennedy J L, *et al.* Modern microwave methods in solid-state inorganic materials chemistry: from fundamentals to manufacturing [J]. *Chem Rev*, 2014, **114**(2): 1170-1206.
[20] Sun Z, Li T, Li G, *et al.* Specific microwave effect on Sn- and Ti-MFI zeolite synthesis [J]. *RSC Adv*, 2017, **7**(56): 35252-35256.
[21] Kim S K, Reddy B M, Park S E. High-performance microwave synthesized mesoporous TS-1 zeolite for catalytic oxidation of cyclic olefins [J]. *Ind Eng Chem Res*, 2018, **57**(10): 3567-3574.
[22] Lamberti C, Bordiga S, Zecchina A, *et al.* Ti location in the MFI framework of Ti-Silicalite-1: A neutron powder diffraction study [J]. *J Am Chem Soc*, 2001, **123**(10): 2204-2213.
[23] Yang Y, Ding J,Xu C, *et al.* An insight into crystal morphology-dependent catalytic properties of MOR-type titanosilicate in liquid-phase selective oxidation [J]. *J Catal*, 2015, **325**: 101-110.
[24] Zhuo Z, Wu L, Wang L, *et al.* Lewis acidic strength controlled highly selective synthesis of oxime via liquid-phase ammoximation over titanosilicates [J]. *RSC Adv*, 2014, **4**(99): 55685-55688.
[25] Wu M,Liu X, Wang Y, *et al.* Synthesis and catalytic ammoxidation performance of hierarchical TS-1 prepared by steam-assisted dry gel conversion method: The effect of TPAOH amount [J]. *J Mater Sci*, 2014, **49**(12): 4341-4348.
[26] Hwang Y K, Lee U H, Chang J S, *et al.* Microwave-induced fabrication of MFI zeolite crystal films onto various metal oxide substrates [J]. *Chem Lett*, 2005, **34**(12): 1596-1597.
[27] Hu P, Yuan F, Bai L, *et al.* Plasma synthesis of large quantities of zinc oxide nanorods [J]. *J Phy Chem C*, 2007, **1**(111): 194-200.
[28] Xu L, Lv G, Li H, *et al.* Surface-modified TS-1 with enhanced activity for cyclohexanone ammoximation in pickering emulsion and increased stability in hot aqueous ammonia [J]. *RSC Adv*, 2015, **5**: 62652-62658.
[29] Wilde N, Worch C, Suprun W, *et al.* Epoxidation of biodiesel with hydrogen peroxide over Ti-containing silicate catalysts [J]. *Micro Mes Mater*, 2012, **164**: 182-189.
[30] Prodinger S, Derewinski M A, Vjunov A, *et al.* Improving stability of zeolites in aqueous phase via selective removal of structural defects [J], *J Am Chem Soc*, 2016, **138**(13): 4408-4415.
[31] Vayssilov G. Structural and physicochemical features of titanium silicalites [J]. *Catal Rev*, 1997, **39**(3): 209-251.
[32] Xia C, Lin M,Zheng A, *et al.* Irreversible deactivation of hollow TS-1 zeolite caused by the formation of acidic amorphous TiO_2-SiO_2 nanoparticles in a commercial cyclohexanone ammoximation process [J]. *J Catal*, 2016, **338**: 340-348.
[33] Lu T,Zou J, Zhan Y, *et al.* Highly efficient oxidation of ethyl lactate to ethyl pyruvate catalysed by TS-1 under mild conditions [J]. *ACS Catal*, 2018, **8**(2): 1287-1296.
[34] Luo Y C, Xiong J H, Pang C L, *et al.* Direct hydroxylation of benzene to phenol over TS-1 catalysts [J]. *Catal*, 2018, **8**(2): 2-14.
[35] Liu M Q, Xiao Z S, Dai J, *et al.* Manganese-containing hollow TS-1: Description of the catalytic sites and surface properties for solvent -free oxidation of ethylbenzene [J]. *Chem Eng J*, 2017, **313**: 1382-1395.
[36] Gao X, An J G, Gu J L, *et al.* A green template-assisted synthesis of hierarchical TS-1 with excellent catalytic activity and recyclability for the oxidation of 2,3,6-trimethylphenol [J]. *Micr Mes Mater*, 2017, **239**: 381-389.
[37] Delmotte L, Soulard M, Guth F, *et al.* ^{19}F MAS NMR studies of crystalline microporous solids synthesized in the fluoride medium [J]. *Zeolites*, 1990, **10**(8): 778-783.
[38] Tekla J, Tarach K A, Olejniczak Z, *et al.* Effective hierarchization of TS-1 and its catalytic performance in cy-

clohexene epoxidation [J]. *Micro Mes Mater*, 2016, **223**: 16-25.

[39] Lu S, Deng X, Liu Y. Synthesis and catalytic oxidation performance of Al-TS-1 [J]. *Chin J Catal*, 2013, **34**: 1232-1241.

[40] Fang X, Wu L, Yu Y, *et al.* Improving the catalytic performance of TS-1 through $Zn(Ac)_2$ modification [J]. *Catal Commun*, 2018, **114**: 1-5.

[41] Wu L, Deng X, Zhao S, *et al.* Synthesis of a highly active oxidation catalyst with improved distribution of titanium coordination states [J]. *Chem Commun*, 2016, **52** (56): 8679-8682.

[42] Wang W, Fu Y, Guo Y, *et al.* Preparation of lamellar-stacked TS-1 and its catalytic performance for the ammoximation of butanone with H_2O_2 [J]. *J Mater Sci*, 2018, **53**(6): 4034-4045.

[43] Wang Y, Liu Y, Li X, *et al.* Intermolecular condensation of ethylenediamine to 1,4-diazabicyclo[2,2,2]octane over TS-1 catalysts [J]. *J Catal*, 2009, **266**(2): 258-267.

[44] Xu L, Ding J, Yang Y, *et al.* Distinctions of hydroxylamine formation and decomposition in cyclohexanone ammoximation over microporous titanosilicates [J]. *J Catal*, 2014, **309**: 1-10.

[45] Bhaumik A, Tatsumi T. Selective dihydroxylation over titanium silicate molecular sieves [J]. *J Catal*, 1998, **176** (2): 305-309.

[46] DengX, Wang Y, Shen L, *et al.* Low-cost synthesis of titanium silicalite-1 (TS-1) with highly catalytic oxidation performance through a controlled hydrolysis process [J]. *Ind Eng Chem Res*, 2013, **52**(3): 1190-1196.

[47] Lu X Q, Zhou W J, Guan Y J, *et al.* Enhancing ethyleneepoxidation of MWW-type titanosilicate/H_2O_2 catalytic system by fluorine implanting [J]. *Catal Sci Technol*, 2017, **7**: 2624-2631.

[48] Mekhemer G A H, Nohman A K H, Fouad N E, *et al.* Surface to bulk characterization of phosphate modified aluminas [J]. *Coll Surf A*, 2000, **161**(3): 439-446.

[49] Noda L K, Almeida R M, Goncalves N S, *et al.* TiO_2 with a high sulfate content thermogravimetric analysis, determination of acid sites by infrared spectroscopy and catalytic activity [J]. *Catal Today*, 2003, **85**(1): 69-74.

[50] Lorenzo D, Romero A, Santos A. A simplified overall kinetic model for cyclohexanone oximation by hydroxylamine salt [J]. *Ind Eng Chem Res*, 2016, **55** (23): 6586-6594.

微波法合成氟改性 TS-1 及其催化环己酮氨肟化性能

薛晓璐[1], 高鹏飞[1], 张 磊[1], 赵永祥[2]

(1. 山西大学 化学化工学院, 山西 太原 030006;
2. 山西大学 精细化学品教育部工程研究中心, 山西 太原 030006)

摘要: 通过微波辅助法制备了含氟的 TS-1(F-TS-1-M), 并与传统方法制备的氟改性 TS-1(F-TS-1-T), 微波处理的 TS-1(TS-1-M)和未改性 TS-1 进行比较. XRD、DR UV-Vis、XPS 表明 F-TS-1-M 和 TS-1-M 分子筛上的部分非骨架钛转变为骨架钛, 这是由于微波的选择性效应可以不同程度地活化 Ti—O 和 Si—O 键; ^{19}F MAS NMR 证实了 F-TS-1-M 分子筛中氟元素是以 Si-F 和 SiF_6^{2-} 的形式存在; ^{29}Si MAS NMR 表明 F-TS-1-M 分子筛的骨架缺陷位和表面羟基减少, Py-FT-IR 结果表明 F-TS-1-M 的 Lewis 酸性和疏水性高于 F-TS-1-T、TS-1-M 和 TS-1. 在环己酮氨肟化的反应中表现出优异的催化性能.

关键词: 氟改性 TS-1; 微波辐射; 路易斯酸; 疏水性; 氨肟化